ARTICLE

High Precision Cavity Ring Down Spectroscopy of $6\nu_3$ Overtone Band of $^{14}N_2{}^{16}O$ near 775 nm

Xiao-qin Zhao[a], Jin Wang[a], An-wen Liu[a]*, Ze-yi Zhou[b], Shui-ming Hu[a]

a. Hefei National Laboratory for Physical Science at the Microscale, University of Science and Technology of China, Hefei 230026, China
b. National Institute of Metrology, Beijing 100013, China

(Dated: Received on May 26, 2017; Accepted on July 12, 2017)

Transitions of the $6\nu_3$ overtone band of $^{14}N_2{}^{16}O$ near 775 nm have been studied by continuous-wave cavity ring-down spectroscopy. Line positions and intensities were derived from a fit of the line shape using a hard-collisional profile. The line positions determined with absolute accuracy of 5×10^{-4} cm^{-1} allowed us to reveal finer ro-vibrational couplings taking place after $J>14$ except a strong anharmonic interaction identified by the effective Hamiltonian model. The absolute line intensities have also been retrieved with an estimated accuracy of 2% for a majority of the unblended lines. A new set of ro-vibrational and dipole moment parameters were derived from the experimental values. A comparison between the line positions and intensities of the $6\nu_3$ band obtained in this work and those from previous studies is given.

Key words: Nitrous oxide, Cavity ring-down spectroscopy, Vibration-rotation spectroscopy

I. INTRODUCTION

Nitrous oxide is a greenhouse gas in the atmosphere with a concentration of about 300 ppbv (part-per-billion in volume). It has become the dominant ozone-depleting substance emitted in the 21st century [1]. Accurate spectroscopic parameters, including positions, intensities, pressure-induced shifts, and broadening coefficients are required for remote-sensing missions [2, 3], the studies of the atmospheres of exoplanets [4, 5], and trace species detection [6]. The spectra of the main isotopologue $^{14}N_2{}^{16}O$ have been systematically studied up to 669 nm with Fourier-transform spectroscopy (FTS) [7−11], intra-cavity laser absorption spectroscopy (ICLAS) [11−16], and cavity ring-down spectroscopy (CRDS) [17−20]. Furthermore, the line positions of $^{14}N_2{}^{16}O$ in the 0−9700 cm^{-1} region can be reproduced with an RMS value of 0.00423 cm^{-1} by a global modeling program using the polyad model of effective Hamiltonian [21]. All line intensities in the range of 0−11000 cm^{-1} can be calculated with the effective dipole moment parameters [9]. However, the accuracy of some line parameters of $^{14}N_2{}^{16}O$ is limited to 20% due to the lack of high precise spectroscopy measurement [22].

Here we present a quantitative study of the $6\nu_3$ overtone band of the main isotopologue of nitrous oxide near 775 nm, using a cavity ring-down spectrometer with high precision as well as high sensitivity. This spectrometer has been previously used to study the extremely weak 6-0 band of carbon monoxide [23] and to determine the absolute frequency of water transitions with an accuracy of about 5 MHz in the 782−840 nm regions [24]. This work is the continuation of a series devoted to the systematic study of high precision absorption spectrum of atmospheric interest species above 1 μm in our laboratory [25, 26]. Line positions and intensities were derived by fitting the recorded spectra with a hard-collisional profile. Investigation of the ground state combination differences confirms that the accuracy of upper level energies is about 5×10^{-4} cm^{-1}, which is over 20 times better than those in previous studies. The improved precision also allows us to find-finer ro-vibrational couplings taking place after $J>14$.

II. EXPERIMENTS

The configuration of the continuous-wave (CW) cavity ring-down spectrometer based on a Ti:Sapphire laser has been presented elsewhere in detail [27−29], and the experimental configuration is similar to that used in our previous studies of the overtone transitions of H_2 [26], CO_2 [25] and CO [23]. The ring-down cavity is about 1 m long and sealed with conflat flanges. The cavity mirrors (Layertec GmbH) have a reflectivity of 99.995% and can be precisely adjusted by a set of step-motors (New Focus Picomotor) by a controller outside the chamber. The ring-down signal is detected by a

*Author to whom correspondence should be addressed. E-mail: awliu@ustc.edu.cn, Tel.: +86-551-63607632

photo-diode and recorded by an analog-digital converter (ADLink PCI 9228). A nonlinear least-square fitting program is applied to fit the data to derive the ring-down time τ. The sample absorption coefficient α at the frequency ν is obtained using the equation:

$$\alpha(\nu) = \frac{1}{c\tau(\nu)} - \frac{1}{c\tau_0} \quad (1)$$

where c is the speed of light and τ_0 is the ring-down time of the empty cavity. The typical noise-equivalent absorption coefficient is 5×10^{-10} cm^{-1}.

The spectrum is calibrated using the longitudinal modes of a 10-cm-long Fabry-Pérot interferometer (FPI) made of ultra-low-expansion (ULE) glass. The ULE-FPI (ATFilms Inc.) is thermal-stabilized at about 302 K and installed in a vacuum chamber. Atomic lines of ^{87}Rb at 780 nm [30] and 795 nm [31], and of ^{133}Cs at 852 nm [32], are used as absolute frequency references. The frequencies of the longitudinal modes of the ULE-FPI are used to calibrate the observed spectrum with an uncertainty better than 10 MHz in the range of 760−850 nm where the group-delay-dispersion of the interferometer is negligible [29, 33].

The $6\nu_3$ band of $^{14}N_2{}^{16}O$ in the 775.2−781.1 nm region were recorded at room temperature. Natural nitrous oxide gas with a stated purity of 99% was bought from Nanjing Special Gas Co. and further purified by a "freeze-pump-thaw" process before use. Different pressures between 15−50 kPa were used in the experiments. The sample pressure was measured by a capacitance gauge (Shanghai ZhenTai CPCA-140Z; full range 100 kPa) with a stated accuracy of 0.5%. An example of the spectra, the P(15) line at 12874.2009 cm^{-1} recorded with a pressure of 50 kPa is presented in FIG. 1 (a).

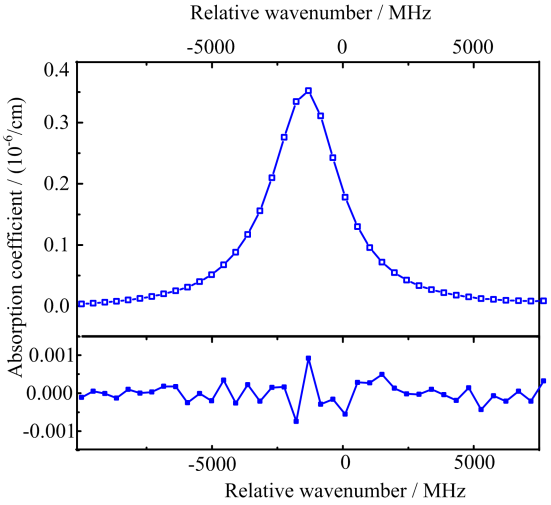

FIG. 1 (a) P(15) line at 12874.2001 cm^{-1} of the $6\nu_3$ band recorded with N_2O samples of 50 kPa. (b) Fitting residuals of the spectrum using a Rautian profile function.

III. RESULTS AND DISCUSSION

A. Transition lists

A "hard" collisional Rautian profile [34] has been applied to fit the spectra recorded at different pressures. The Gaussian width was fixed at the calculated Doppler broadening width. Since the Dicke narrowing parameters derived from fit of the spectra are not physically reasonable in most cases, the narrowing parameters β were also fixed at the values given by the diffusion theory following the relation [35],

$$\beta = \frac{k_B T}{2\pi m c D} \quad (2)$$

where k_B is the Boltzmann constant, T is the temperature, m is the molecular mass of N_2O, c is the speed of light, and D is the mass-diffusion coefficient of N_2O, which can be calculated from Lennard-Jones intermolecular potential parameters [36]. Other line parameters, including the position, intensity, Lorentzian width (half-width at half-maximum) were obtained from the fit. For illustration, FIG. 1(b) shows the fitting residuals of the P(15) line recorded at 50 kPa. The line position at the zero pressure limit and the line intensity were derived by using a linear fit. The results from 87 lines are collected in Table I together with the statistical uncertainties obtained from the fit. Note that the line positions of 44 transitions recorded with only two different pressures were given without uncertainties. The combination differences between the transitions reaching the same upper level for the unblended lines are below 5×10^{-4} cm^{-1}, being consistent with the experimental accuracy.

B. Spectroscopic constants of the upper states

The ro-vibrational energies of $6\nu_3$ state of $^{14}N_2{}^{16}O$ can be expressed with the standard energy level equation:

$$E_v(J) = G_v + B_v J(J+1) - D_v J^2(J+1)^2 + H_v J^3(J+1)^3 \quad (3)$$

where G_v is the vibrational term value, B_v is the rotational constant, D_v and H_v are centrifugal distortion constants, J is the angular momentum quantum number. The spectroscopic parameters for an upper state were fitted directly to the observed line positions listed in Table I. The ground state rotational constants were constrained to the literature values [37]. A resonance anharmonic interaction between the 00^06 and 04^05 vibrational states at J'=65 and the perturbation by the 04^25 vibration state (anharmonic and l-type interaction) at J'=53 were found on the basis of predictions of the EH model [38, 39] given in Ref.[16]. For this reason, only levels of $J'\leq46$ were included in the fit and

DOI:10.1063/1674-0068/30/cjcp1705109

TABLE I Line positions (in cm^{-1}) and intensities of $6\nu_3$ band of $^{14}N_2{}^{16}O$.

	Position, $\nu_{obs.}$	$S_{expt.}$	%
P(1)	12890.2411*	0.541(3)	9.1
P(2)	12889.3606*	0.963(3)	−2.2
P(3)	12888.44124(15)	1.463(4)	0.3
P(4)	12887.48051(09)	1.905(3)	−0.5
P(5)	12886.47921(12)	2.286(3)	−2.6
P(6)	12885.43677(08)	2.701(2)	−1.7
P(7)	12884.35331(07)	3.080(1)	−1.2
P(8)	12883.22886(09)	3.413(3)	−1.1
P(9)	12882.06328(05)	3.726(3)	−0.5
P(10)	12880.8562*	3.928(5)	−1.7
P(11)	12879.60773(04)	4.319(3)	−2.7
P(12)	12878.31836(08)	4.383(4)	0.2
P(13)	12876.98743(04)	4.471(5)	−0.5
P(14)	12875.61584*	4.674(5)	2.1
P(15)	12874.20098(07)	4.721(7)	2.3
P(16)	12872.74598(05)	4.622(7)	0.1
P(17)	12871.24904(05)	4.649(3)	1.5
P(18)	12869.71121(05)	4.512(3)	0.0
P(19)	12868.13161(09)	4.416(3)	0.1
P(20)	12866.51085(02)	4.292(2)	0.2
P(21)	12864.84837(04)	4.157(4)	0.6
P(22)	12863.14473(07)	3.957(1)	−0.1
P(23)	12861.39956(07)	3.759(2)	−0.4
P(24)	12859.61310(12)	3.591(5)	0.4
P(25)	12857.78563(12)	3.372(3)	0.1
R(0)	12891.8745*	0.483(2)	−3.1
R(1)	12892.6312*	0.972(2)	−2.0
R(2)	12893.3467*	1.484(3)	0.6
R(3)	12894.0208*	1.982(3)	2.0
R(4)	12894.6545*	2.384(5)	−0.2
R(5)	12895.2472*	2.756(6)	−1.9
R(6)	12895.7970*	3.248(8)	1.6
R(7)	12896.3089*	3.497(2)	−1.6
R(8)	12896.7777*	3.916(6)	1.2
R(9)	12897.2047*	4.141(6)	−0.1
R(10)	12897.5880*	4.436(9)	1.4
R(11)	12897.9345*	4.531(9)	−0.8
R(12)	12898.2368*	4.589(10)	−2.6
R(13)	12898.4977*	5.10(73)	6.0
R(14)	12898.7224*	5.78(15)	18.6
R(15)	12898.9038*	5.86(32)	19.8

the resulted spectroscopic parameters are given in Table II (row "a"). The spectroscopic constants derived from the fit of the ICLAS data [16] are also included in Table II. As shown in the upper panel of FIG. 2, the ro-vibrational energy levels calculated from the "a" set of parameters can reproduce the experimental values

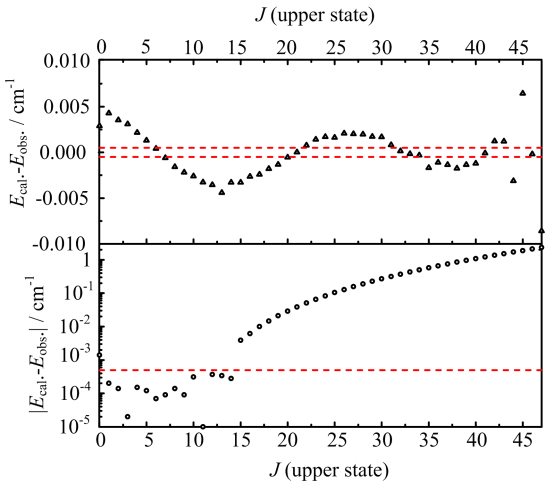

FIG. 2 Difference between the observed energy levels of the $6\nu_3$ state of $^{14}N_2{}^{16}O$ and the calculated values. Upper panel: The "a" set of parameters in Table II were used in the calculation. Lower panel: The "b" set of parameters in Table II were used in the calculation.

within 0.005 cm^{-1}. However, the deviations of some energy levels are about ten times of the experimental uncertainties of line positions. Apparently, the deviations also have a regular dependence on the J' value, which implies that there may exist some unidentified perturbations based on the EH model. The lower panel of FIG. 2 shows the absolute deviations between the observed energies and those calculated from the "b" set of parameters listed in Table II. A perturbation starting at the J'=15 level can be easily identified. The "b" set of spectroscopic parameters were obtained from a fit of the $J'\leq$14 energy levels. The mean deviation of the fit is 1.1×10^{-4} cm^{-1}, being consistent with the experimental uncertainty, which is indicated by a dashed line in FIG. 2. The deviation between the observed and calculated energies has a clear jump at J'=15, from 3×10^{-4} cm^{-1} to 4×10^{-3} cm^{-1}, which indicates a perturbation starting from here. The perturbation is out of the predictive ability of the EH model or the lower precision spectrum. Note that a similar phenomenon has been found in the $4\nu_{CH}$ overtone of $^{12}C_2H_2$ [40].

C. Vibrational transition dipole moment squared and Herman-Wallis factor

The line strength $S(T_0)$ in $cm^{-1}/(cm^{-2}\cdot mol)$ at the standard temperature T_0=296 K can be deduced using the following equation:

$$S(T_0) = \frac{1}{4\pi\varepsilon_0}\frac{8\pi^3 v_0 C}{3hcQ(T_0)}|R|^2 L(J,l)e^{-hcE/k_BT_0}\left(1-e^{-hcv_0/kT_0}\right) \quad (4)$$

DOI:10.1063/1674-0068/30/cjcp1705109

TABLE II Spectroscopic constants (in cm^{-1}), vibrational transition moments $|R_v|^2$ (in D^2), Herman-Wallis parameters of the $6\nu_3$ band of $^{14}N_2{}^{16}O$ in the present study.

	G_v	B_v	$D_v\times10^7$	$H_v\times10^{11}$	$J_{\rm incl}/J_{\rm max}$	n/N	rms	$\lvert R\rvert^2\times10^{11}$	$A_1\times10^4$	$A_2\times10^6$
G.S.	0.0	0.419011001	1.7609193	−0.016529						
a	12891.081962(43)	0.39848502(25)	3.2265(32)	6.139(11)	47/48	86/87	2.3	4.598(16)	−1.52(44)	9.0(19)
b	12891.077683(76)	0.3985913(21)	6.86(11)		14/48	24/87	0.11			
c	12891.0869(18)	0.398417(62)	1.748(38)		41/48	81/95	8.5			
d	12891.0766(12)	0.3985044(32)	3.446(16)	6.935(76)	48/48	90/95	5.7	1.658(11)		

G.S.: ground vibrational state.
a: this work, from a fit of the upper-level energies $J'\leq46$.
b: this work, from a fit of the upper-level energies $J'\leq14$.
c: Ref.[16], fit without H_v.
d: Ref.[16], fit with H_v.
rms: root mean square deviation in 10^{-3} cm^{-1}.

In Eq.(4), $1/4(\pi\varepsilon_0)=10^{-36}$ ergcm^{3}D^{-2}, h is Planck's constant, c is the vacuum speed of light, v_0 is the transition wavenumber in cm^{-1}, C=0.990331 is the isotopic abundance of $^{14}N_2{}^{16}O$, $Q(T_0)$ is the total partition function at temperature T_0, $L(J,l)$ is the Hönl-London factor, J is the rotational quantum number of the lower state of the transition and l is the quantum number of the projection of the vibrational angular momentum on the molecular axis, E'' in cm^{-1} is the energy of the lower level, k_B is the Boltzmann constant.

For the $6\nu_3$ band of $^{14}N_2{}^{16}O$, the Hönl-London factor $L(J,l)$ is equal to $|m|$, where m is $-J$ for the P branch, and J+1 for the R branch. For the isolated vibrational state of a linear molecule, the rotational dependence of the transition dipole moment squared can be expressed by the well-known expression:

$$|R|^2 = |R_0|^2(1 + A_1m + A_2m^2)^2 \qquad (5)$$

where $|R_0|^2$ is the vibrational transition dipole moment squared, and A_1, A_2 are the Herman-Wallis coefficients. $|R_0|^2$ values and the Herman-Wallis coefficients obtained from an unweighted fit of the $|R|^2$ values of 73 unblended lines are given in Table II. FIG. 3 presents the transition dipole moment squared versus rotational quantum number m. The relative differences between experimental and calculated intensities with this set of Herman-Wallis coefficients are given in Table I. The relative deviations are less than 2% for well-isolated lines.

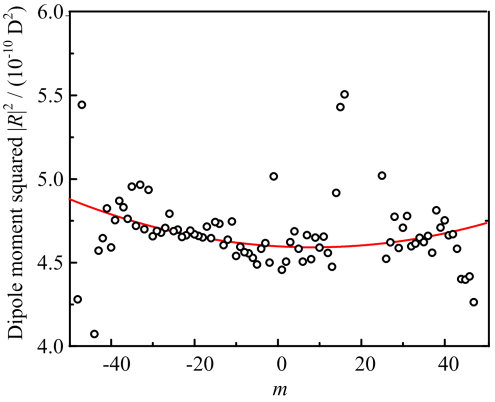

FIG. 3 Experimental (open circle) and calculated (solid line) values of the transition dipole moment squared of the $6\nu_3$ bands of $^{14}N_2{}^{16}O$. The calculated values of $|R|^2$ are obtained using the parameters given in Table II.

D. Comparison of the experimental line positions and intensities

The experimental line positions and intensities of $6\nu_3$ band of $^{14}N_2{}^{16}O$ have been determined by Milloud *et al.* using ICLAS [16]. The ICLAS N_2O line positions were calibrated by an intra-cavity etalon and the H_2O reference lines taken from HITRAN2008 [41], and the uncertainty for the positions of well isolated lines was estimated to be 0.01 cm^{-1}, which is twenty times worse than this work. The upper panel of FIG. 4 shows the line position deviations from this work to ICLAS. The absolute deviations of most lines are within 0.01 cm^{-1}, consistent with the ICLAS uncertainty.

Although ICLAS is also very sensitive, due to the interference from atmospheric water absorption around 775 nm, the uncertainty of ICLAS line intensities was claimed to be within 11%, over 5 times worse than this work. A comparison of the line intensities between CRDS and ICLAS measurements is plotted in the lower panel of FIG. 4. In average, our CRDS intensities are 30% larger than the ICLAS values. We believe that the new experimental results presented in this work will help for further improvement of the effective dipole moment parameter M_{006} [16].

IV. CONCLUSION

New experimental data on the ro-vibrational transitions of nitrous oxide near 775 nm have been obtained

DOI:10.1063/1674-0068/30/cjcp1705109

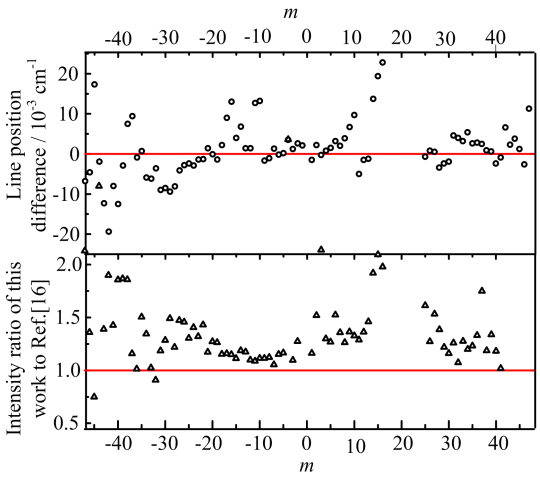

FIG. 4 Comparison of the experimental line position and intensity of the $6\nu_3$ band of $^{14}N_2{}^{16}O$ between this work and Ref.[16]. Upper panel: deviation of the line positions from this work to Ref.[16], lower panel: ratio of the line intensities between this work and Ref.[16].

with a continuous-wave cavity ring-down spectrometer using a Ti:Sapphire laser. Line positions have been determined with an accuracy of 5×10^{-4} cm^{-1}, and line intensities are determined with a relative uncertainty of about 2% for not-too-weak and unblended lines. Improved sets of rovibrational and dipole moment parameters were determined with new experimental data. The improved precision provides an insight of the intramolecular perturbation taking place after J>14. The new data presented here will be used to refine the effective dipole moment parameter of $^{14}N_2{}^{16}O$.

V. ACKNOWLEDGMENTS

This work was supported by the National Key Basic Research Program of China (2013CB834602 and 2013BAK12B02), and the National Natural Science Foundation of China (No.21473172, No.21411130183, No.21303176).

[1] A. R. Ravishankara, J. S. Daniel, and R. W. Portmann, Science **326**, 123 (2009).
[2] D. R. Thompson, D. C. Benner, L. R. Brown, D. Crisp, V. M. Devi, and Y. B. Jiang, J. Quant. Spectrosc. Radiat. Transfer **113**, 2265 (2012).
[3] A. V. Nikitin, O. M. Lyulin, S. N. Mikhailenko, V. I. Perevalov, N. N. Filippov, I. M. Grigoriev, I. Morino, T. Yokota, R. Kumazawa, and T. Watanabe, J. Quant. Spectrosc. Radiat. Transfer **111**, 2211 (2010).
[4] B. Bezard, A. Fedorova, J. L. Bertaux, A. Rodin, and O. Korablev, Icarus, **216**, 173 (2011).
[5] P. Hedelt, P. von Paris, M. Godolt, S. Gebauer, J. L. Grenfell, H. Rauer, F. Schreier, F. Selsis, and T. Trautmann, Astron. Astrophys. **553**, A9 (2013).
[6] N. G. Phillips, R. Ackey, E. R. Crosson, A. Down, L. R. Hutyra, M. Brondfield, J. D. Karr, K. G. Zhang, and R. B. Jackson, Environ. Pollut. **173**, 1 (2013).
[7] L. Daumont, J. Vander Auwera, J. L. Teffo, V. I. Perevalov, and S. A. Tashkun, J. Mol. Spectrosc. **208**, 281 (2001).
[8] L. Daumont, C. Claveau, M. R. Debacker-Barilly, A. Hamdouni, L. R. Regalia-Jarlot, J. L. Teffo, S. A. Tashkun, and V. I. Perevalov, J. Quant. Spectrosc. Radiat. Transfer **72**, 37 (2002).
[9] L. Daumont, J. Vander Auwera, J. L. Teffo, V. I. Perevalov, and S. A. Tashkun, J. Quant. Spectrosc. Radiat. Transfer **104**, 342 (2007).
[10] L. Wang, V. I. Perevalov, S. A. Tashkun, B. Gao, L. Y. Hao, and S. M. Hu, J. Mol. Spectrosc. **237**, 129 (2006).
[11] G. Weirauch, A. A. Kachanov, A. Campargue, M. Bach, M. Herman, and J. Vander Auwera, J. Mol. Spectrosc. **202**, 98 (2000).
[12] A. Campargue, G. Weirauch, S. A. Tashkun, V. I. Perevalov, and J. L. Teffo, J. Mol. Spectrosc. **209**, 198 (2000).
[13] E. Bertseva, A. A. Kachanov, and A. Campargue, Chem. Phys. Lett. **351**, 18 (2002).
[14] Y. Ding, V. I. Perevalov, S. A. Tashkun, J. L. Teffo, E. Bertseva, and A. Campargue, J. Mol. Spectrosc. **220**, 80 (2003).
[15] E. Bertseva, A. Campargue, V. I. Perevalov, and S. A. Tashkun, J. Mol. Spectrosc. **226**, 196 (2004).
[16] R. Milloud, V. I. Perevalov, S. A. Tashkun, and A. Camparuge, J. Quant. Spectrosc. Radiat. Transfer **112**, 553 (2011).
[17] A. W. Liu, S. Kassi, P. Malara, D. Romanini, V. I. Perevalov, S. A. Tashkun, S. M. Hu, and A. Campargue, J. Mol. Spectrosc. **244**, 33 (2007).
[18] A. W. Liu, S. Kassi, V. I. Perevalov, S. A. Tashkun, and A. Campargue, J. Mol. Spectrosc. **244**, 48 (2007).
[19] A. W. Liu, S. Kassi, V. I. Perevalov, S. M. Hu, and A. Campargue, J. Mol. Spectrosc. **254**, 20 (2009).
[20] A. W. Liu, S. Kassi, V. I. Perevalov, S. A. Tashkun, and A. Camparuge, J. Mol. Spectrosc. **267**, 191 (2011).
[21] V. I. Perevalov, S. A. Tashkun, R. V. Kochanov, A. W. Liu, and A. Campargue, J. Quant. Spectrosc. Radiat. Transfer **113**, 1004 (2012).
[22] L. S. Rothman, I. E. Gordon, Y. Babikov, A. Barbe, D. Chris Benner, P. F. Bernath, M. Birk, L. Bizzocchi, V. Boudon, L. R. Brown, A. Campargue, K. Chance, E. A. Cohen, L. H. Coudert, V. M. Devi, B. J. Drouin, A. Fayt, J. M. Flaud, R. R. Gamache, J. J. Harrison, J. M. Hartmann, C. Hill, J. T. Hodges, D. Jacquemart, A. Jolly, J. Lamouroux, R. J. Le Roy, G. Li, D. A. Long, O. M. Lyulin, C. J. Mackie, S. T. Massie, S. Mikhailenko, H. S. P. Mller, O. V. Naumenko, A. V. Nikitin, J. Orphal, V. Perevalov, A. Perrin, E. R. Polovtseva, C. Richard, M. A. H. Smith, E. Starikova, K. Sung, S. Tashkun, J. Tennyson, G. C. Toon, VI. G. Tyuterev, and G. Wagner, J. Quant. Spectrosc. Radiat. Transfer **130**, 4 (2013).
[23] Y. Tan, J. Wang, X. Q. Zhao, A. W. Liu, and S. M. Hu, J. Quant. Spectrosc. Radiat. Transfer **187**, 274 (2017).
[24] S. M. Hu, B. Chen, Y. Tan, J. Wang, C. F. Cheng, and

A. W. Liu, J. Quant. Spectrosc. Radiat. Transfer **164**, 37 (2015).
[25] Y. Lu, A. W. Liu, X. F. Li, J. Wang, C. F. Cheng, Y. R. Sun, and R. Lambo, and S. M. Hu, Astrophys. J. **775**, 71 (2013).
[26] S. M. Hu, H. Pan, C. F. Cheng, Y. R. Sun, X. F. Li, J. Wang, A. Campargue, and A. W. Liu, Astrophys. J. **749**, 76 (2012).
[27] B. Gao, W. Jiang, A. W. Liu, Y. Lu, C. F. Cheng, G. S. Cheng, and S. M. Hu, Rev. Sci. Instrum. **81**, 043105 (2010).
[28] H. Pan, C. F. Cheng, Y. R. Sun, B. Gao, A. W. Liu, and S. M. Hu, Rev. Sci. Instrum. **82**, 103110 (2011).
[29] C. F. Cheng, Y. R. Sun, H. Pan, Y. Lu, X. F. Li, J. Wang, A. W. Liu, and S. M. Hu, Opt. Expr. **20**, 9956 (2012).
[30] J. Ye, S. Swartz, P. Jungner, and J. L. Hall, Opt. Lett. **21**, 1280 (1996).
[31] M. Maric, J. J. McFerran, and A. N. Luiten, Phys. Rev. A **77**, 032502 (2008).
[32] T. Udem, J. Reichert, T. W. Hänsch, and M. Kourogi, Phys. Rev. A **62**, 031801 (2000).
[33] Y. Tan, J. Wang, C. F. Cheng, X. Q. Zhao, A. W. Liu, and S. M. Hu, J. Mol. Spectrsc. **300**, 60 (2014)
[34] S. G. Rautian and I. I. Sobel'man, Sov. Phys. Usp. Engl. Transl. **9**, 701 (1967).
[35] M. Lepère, Spectrochim. Acta Part A **60**, 3249 (2004).
[36] J. O. Hirschfelder, C. F. Curtiss, and R. B. Bird, *Molecular Theory of Gases and Liquids*, New York: Wiley, (1967).
[37] R. A. Toth, J. Mol. Spectrosc. **197**, 158 (1999).
[38] J. L. Teffo, V. I. Perevalov, and O. M. Lyulin, J. Mol. Spectrosc. **168**, 390 (1994).
[39] V. I. Perevalov, S. A. Tashkun, and J. L. Teffo, *Sixteenth Colloquium on High Resolution Molecular Spectroscopy*, Dijion, France, 6-10 September 103 (1999).
[40] A. W. Liu, X. F. Li, J. Wang, Y. Lu, C. F. Cheng, Y. R. Sun, and S. M. Hu, J. Chem. Phys. **138**, 014312 (2013).
[41] L. S. Rothman, I. E. Gordon, A. Barbe, D. Chris Benner, P. F. Bernath, M. Birk, V. Boudon, L. R. Brown, A. Campargue, J. P. Champion, K. Chance, L. H. Coudert, V. Dana, V. M. Devi, S. Fally, J. M. Flaud, R. R. Gamache, A. Goldman, D. Jacquemart, I. Kleiner, N. Lacome, W. J. Lafferty, J. Y. Mandin, S. T. Massie, S. N. Mikhailenko, C. E. Miller, N. Moazzen-Ahmadi, O. V. Naumenko, A. V. Nikitin, J. Orphal, V. I. Perevalov, A. Perrin, A. Predoi-Cross, C. P. Rinsland, M. Rotger, M. Simeckova, M. A. H. Smith, K. Sung, S. A. Tashkun, J. Tennyson, R. A. Toth, A. C. Vandaele, and J. Vander Auwera, J. Quant. Spectrosc. Radiat. Transfer **110**, 533 (2009).

DOI:10.1063/1674-0068/30/cjcp1705109